Statistical Analysis of 100 Gbps per Wavelength SWDM VCSEL-MMF Data Center Links on a Large Set of OM3 and OM4 Fibers

Statistical Analysis of 100 Gbps per Wavelength SWDM VCSEL-MMF Data Center Links on a Large Set of OM3 and OM4 Fibers

Pablo Torres-Ferrera, Giuseppe Rizzelli, Antonino Nespola, Jose M. Castro, Bulent Kose, Fabrizio Forghieri, Roberto Gaudino, *Senior Member, IEEE* and Andrea Carena, *Senior Member, IEEE*

***Abstract*—We present a detailed statistical study on achievable reach of 100 Gbps data center optical links based on vertical cavity surface emitting lasers (VCSEL) and multimode fibers (MMF). Based on the characterization of the spectral and spatial properties of eight lasers and of the modal and dispersion behavior of a large set of 20233 OM3 and OM4 modeled fibers (obtained by properly extending an initial set of 500 measured fibers), we compute the resulting frequency responses of all of the VCSEL-MMF combinations. Then, we feed them to a numerical tool modeling PAM-4 transmission at 100 Gbps net bit rate per wavelength. Our model analyzes performance at distances up to 400 meters, using three different adaptive equalizers at the receiver and considering two forward error correction overheads. We show that 100 Gbps operation is feasible for 99% of the simulated links reaching up to 120 m over OM4 at 850 nm and using a decision feedback equalizer (DFE). Aggregated data rates of 200 Gbps and 400 Gbps per fiber using Shortwave Wavelength Division Multiplexing (SWDM) are achievable for 99% of the links reaching 80 m over OM4 using two wavelengths and feed-forward equalizer (FFE) and four wavelengths and maximum likelihood sequence estimation (MLSE)-based equalizer, respectively.**

***Index Terms*—Multimode Fibers, Shortwave Wavelength Division Multiplexing (SWDM), Vertical Cavity Surface Emitting Lasers (VCSEL), Digital Signal Processing (DSP), PAM-4.**

I. Introduction

SHORT-REACH links over MMF using directly modulated VCSEL-based transceivers are the most widely deployed solution in enterprise data centers interconnects (DCI) when distances to be covered are in the order of hundreds of meters, due to their advantages with respect to single-mode systems [1], such as:

- VCSELs cost-effectiveness in terms of manufacturability, integration, reliability and power consumption;
- MMF large core that simplifies fiber alignment and therefore reduces total transceiver cost;
- MMF connections that require less stringent geometrical specifications.

Nowadays, VCSEL-MMF DCI commercial solutions, defined in Ethernet 100GBASE-SR4 and Fiber Channel (FC) 32G-FC standards, are able to transmit up to 28 Gbps per lane over 70 m and 100 m using OM3 and OM4 fibers, respectively. On-off keying (OOK) is used as modulation format, without pre- or post-equalization, in combination with RS-FEC(544, 514). The intensity modulation (IM) and direct detection (DD) approach is employed using 25G-class devices (i.e. optoelectronic that is "natively" suitable for 25 Gbps OOK).

Recent traffic increase driven by modern technologies and services such as 5G, Internet of Things, cloud services, among others, is continuously posing the challenge of upgrading DCI capacity above their current limit. On top of the bandwidth limitations of the optoelectronic devices, Modal Dispersion (MD) and Chromatic Dispersion (CD) set a cap to the maximum achievable data rate and reach of current MMF systems [2-5]. According to [4] and [5], a -3 dB bandwidth of around 20 GHz is estimated for 70 m OM3 and 100 m OM4 fibers. Therefore, to increase the VCSEL-MMF links capacity beyond 25 Gbps per wavelength (λ), different alternatives should be considered [6]: increasing the modulation efficiency, using multiple λs, including digital signal processing (DSP) equalization, and/or using new broader bandwidth MMFs.

In 2020, the IEEE P802.3cm Task Force completed the definition of 400 Gbps solutions over VCSEL-MMF links [7], transmitting 50 Gbps/λ with (un-equalized) PAM-4 as modulation format, either using 8 fiber-pairs and a single λ per fiber (400GBASE-SR8) or 4 fiber-pairs and two λs per fiber (400GBASE-SR4.2). In both cases, a reach of 100 m over OM4, and 70 m over OM3, was again specified. These standardization efforts are driven by the fact that OM3 and OM4 are the most widely deployed MMF cabling solutions in today's DCI [1, 8], thus paving the way for a smooth transition towards higher data rates at a reduced cost.

Short Wavelength Division Multiplexing (SWDM) was developed as another alternative to enable 100 Gbps per fiber transmission [8-13] using 25 Gbps/λ and 4 wavelengths (850, 880, 910, and 940 nm), with an extended reach of up to 150 m

This work was carried out under the PhotoNext initiative at Politecnico di Torino (http://www.photonext.polito.it/). Some of the computational resources were provided by HPC@POLITO (http://www.hpc.polito.it).

P. Torres-Ferrera, G. Rizzelli, R. Gaudino and A. Carena are with Politecnico di Torino, Department of Electronics and Telecommunications, Torino, Italy (e-mail: pablo.torres@polito.it).

A. Nespola is with LINKS Foundation, Torino, Italy.

J. Castro and B. Kose are with Panduit Laboratories, Orland Park, IL 60467 USA.

F. Forghieri is with CISCO Photonics Italy, Vimercate, Italy

using OM5 [9]. Recent work has demonstrated operative distances up to 250 m using OM5 [10] and 300 m using a new wideband OM4 [11, 12].

Achieving 100 Gbps/λ is the next step in the VCSEL-MMF DCI evolution. This target seems unfeasible using OOK, even if introducing equalization [6]. Recently, OOK transmission up to 80 Gbps and 72 Gbps over 2 m and 50 m, respectively, has been shown [14]. To overcome this limitation, the use of high-order modulation formats and DSP equalization [6], while preserving 25G-class devices, has been analyzed. For instance, 100 Gbps+ transmission has been demonstrated using PAM-4 [3, 5, 6, 15], duobinary PAM-4 [16], discrete multi-tone (DMT) [17], and carrier-less amplitude phase modulation (CAP) [18, 19], reaching at least 100 meters. Currently, standards for bit rates above 50 Gbps/λ are being developed by the Fiber Channel PI-8 and the IEEE 802.3db Task Force that has recently adopted two reach targets for 100 Gbps/λ: 50 m and 100 m [20]. The possibility of reusing the already installed OM3 and OM4 infrastructure (as well as current 25G-class devices) adds to the intrinsic advantages of VCSEL-MMF that have enabled their success in the early stages of DCI development.

To estimate the ultimate limits of 100 Gbps/λ PAM-4 VCSEL-MMF links over OM3 and OM4 fibers, in this paper we report on an extensive statistical performance analysis based on a large dataset including the characterization of 8 VCSELs and 20233 modeled MMFs (16467 OM3 and 3766 OM4) obtained by properly extending an initial set of 500 measured fibers, following an algorithm detailed in sub-section II.A. The characterization was performed at four different λs in order to extend our analysis to a 400 Gbps system implemented as a 4λ x 100 Gbps/λ SWDM solution [6, 21]. Performing a statistical study on such a vast number of link samples is fundamental for VCSEL-MMF based systems, which are known to be affected by random variations. To the best of our knowledge, this is the first study of this type for recent ultra-high bit rate systems (100 Gbps/λ). In particular, thanks to such a large amount of data, we were able to compute the transfer functions of 161864 VCSEL-MMF combinations per λ and per fiber length, through the model presented in [2]. Then, they have been used to simulate PAM-4 transmission based on realistic transceiver parameters considering three different types of receiver with adaptive equalizers. The metric used to define the system performance is the maximum achievable reach at the forward error correction (FEC) threshold: we considered transmission both with a soft KP4-FEC with bit error rate (BER) target (BER_T) of $2{\cdot}10^{-4}$ and a stronger enhanced-FEC (E-FEC) with $BER_T = 4{\cdot}10^{-3}$. Different FECs imply also a different amount of overhead to be considered in physical layer propagation. We intentionally did not use more complex FEC (such as those having BER_T in the order 10^{-2}) since they are perceived as too complex, costly, and power-hungry for the MMF datacenter ecosystem.

The remainder of this paper is organized as follows: in Section II, we present the characterization method of the VCSELs and the OM3 and OM4 MMFs. We also introduce the numerical model employed for MMF transfer function computation and show the inverse cumulative distribution function (i-CDF) of the -3 dB optical (dBo) bandwidth ($B\text{-}_{3dB}$) for some specific VCSEL-MMF combinations. In Section III, we describe the main features of the PAM-4 transmission simulator, including details on the optoelectronic transmitter and receiver model and on the digital signal processing (DSP) functions, focusing on the implementation of three different adaptive equalizers: a feed-forward equalizer (FFE), a decision feedback equalizer (DFE) and a maximum-likelihood sequence estimation (MLSE)-based equalizer. In this Section, we also show the simulation performance in back-to-back (BtB) conditions. Section IV includes the core results of our work, introducing statistics of the maximum achievable transmission distance over the OM3 and OM4 fibers populations for PAM-4-based SWDM systems at 100 Gbps net bit rates per wavelength at the two different FEC thresholds. Lastly, in Section V we summarize the main results and draw some conclusions.

II. VCSEL-MMF Coupling Model

The model for the VCSEL-MMFs channels is described in this Section. In particular, in sub-section II.A we describe the fiber model and its relation with standards method to characterize the channels while in the following sub-section II.B, we describe the coupling model and effects in modal bandwidth.

A. MMF Fiber Population

MMFs used for datacenters or LAN are classified based on their effective modal bandwidth (EMB). The EMB, a metric computed from differential mode delay (DMD) measurements, represents the worst-case bandwidth produced by ten representative VCSEL launch conditions. The minimum EMB values specified in TIA and IEC standards [22, 23] required for selecting OM3 and OM4 at 850 nm are 2.0 GHz-km and 4.7 GHz-km, respectively.

Although the minimum EMB limits are convenient to estimate worst-case performance, they are not sufficient for the statistical analysis of 100 Gbps/λ performance, particularly for receivers using adaptive equalization. The main target of this paper is, in fact, to estimate statistically the feasibility of equalized 100 Gbps/λ and, to this end, we use a dataset of OM3 and OM4 representative fibers generated by DMD modeling and measurements.

The algorithm to generate the fiber datasets is shown in Fig. 1(a). The process starts with DMD experimental measurements of a set of 500 fibers from major suppliers, which become the initial MMF population [24]. The range of fiber lengths for DMD measurements was 300–500 m. From such measurements, EMB distributions and tolerances observed by major fiber suppliers, we estimated distributions for the production of MMF OM3 and OM4.

The performed 500 DMD measurements follow the standard procedure described in [22, 23]. The procedure describes the launch of an optical reference pulse $P_{Ref}(t)$ at several radial positions inside the core of the fiber under test.

For each launch, the optical pulses $P_{\mathrm{DMD}}(t, r)$ that reach the

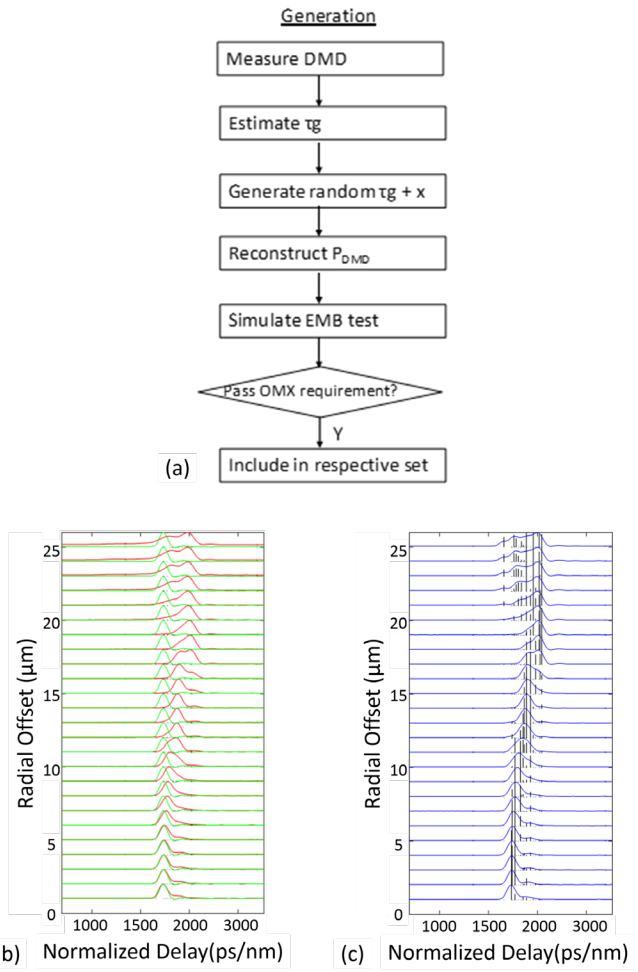

Fig. 1 (a) Methodology for extending the number of element in the MMF dataset, (b) Measured DMD pulses as function of radial offset (red trace) and reference pulses (green trace), (c) Mode groups (black lines) and reconstructed DMD pulses (blue traces).

far end of the fiber under test are measured by a large-area detector. A large area detector is needed to ensure that all the fiber propagating modes were captured. The electrical signal at the receiver output is sent to a sampling scope. Following the DMD procedure [22, 23], the modal bandwidth of the fiber is computed using:

$$H_{MB}^{\{k\}}(f) = \left| FFT\left\{ \sum_{r=1}^{N_r} w_k(r) P_{DMD}(t,r) \right\} / FFT\{P_{\mathrm{Ref}}(t)\} \right| \qquad (1)$$

where $FFT\{.\}$ represents the Fast Fourier Transform operator, $|\cdot|$ the norm operator and N_r the number of radial offsets, which determines the spatial resolution of the measurement. In the experimental data measured for this work, the reference pulse was launched from the center to the edge of the core (±25 microns) in steps of one micron. The term $w_k(r)$ represents the launch condition of the k^{th} VCSEL of a set of ten representatives VCSELs defined in [22].

The -3 dB modal bandwidth for the k^{th} representative VCSELs is obtained from the transfer function shown in Eq. (1) using a Gaussian approximation defined in the standard [22, 23]. The minimum EMB is defined as the lowest modal bandwidth among the ten representative VCSELs.

The method summarized above is currently used to classify multimode fibers in categories such as OM3/OM4 based on the EMB value at 850 nm.

The second step of the procedure shown in Fig. 1(a) estimates the mode group delays τ_g from the DMD measurements by numerically de-convolving the expression of the estimate of the received pulse shape considering all mode group propagating in the MMF fiber:

$$P_{DMD}(t,r) = \left(\sum_{g=1}^{N_g} A_g(r)\delta(t-\tau_g) \right) \otimes P_{Ref}(t,r) \qquad (2)$$

where $A_g(r)$ represents the power of the g^{th} mode group when the reference pulse was launched at position r, τ_g the mode group delays, N_g the maximum number of mode groups at the measured wavelength, $\otimes$ the convolution operator and $\delta(\cdot)$ the delta Dirac function. The metric to discriminate among possible solutions of the numerical de-convolution was the root-mean square (RMS) error between the measured DMD pulses and the reconstructed DMD ones.

An example illustrating the numerical deconvolution method is shown in Fig. 1(b). The figure shows the measured launched reference (green traces) and the received DMD pulses (red traces) for the several radial launch offsets inside the fiber core. Those set of pulses are used in Eq. (2) to numerically obtain $A_g(r)$ and τ_g.

At 850 nm, 19 mode groups are represented by impulses shown in Fig 1(c) (in black lines). The heights of the impulses represent the relative coupled power in each mode group from an offset single mode launch.

To evaluate the accuracy of the solution, $P_{\mathrm{DMD}}(t,r)$ were reconstructed employing the obtained mode parameters and $P_{Ref}(t)$, in Eq. (2). Fig. 1(c) shows the reconstructed DMD pulses (in blue traces).

The procedure described above was repeated for the 500 measured fibers. Once the mode group delays were obtained, the population was expanded randomly producing new mode group vectors.

This step, in the procedure shown in Fig. 1(a), was meant to extend the original experimental 500 fibers dataset to a much larger dataset, by numerically adding random perturbations to the mode group delays with the following rule:

$$\tau'_g = \tau_g(1+x_1) + x_2 \qquad (3)$$

where x_1 and x_2 are zero-mean random variables with Gaussian distribution. Standard deviations are set to 0.06 and 8 ps/km, respectively, to match the original distribution found within the 500 experimentally characterized fibers. The DMD pulses for the new set of mode group delays were computed using Eq. (2) and a measured reference pulse. The generated DMD pulses were used to compute the EMB which was used to classify the new simulated fibers into OM3 or OM4 sets. An overlap of EMB values between the sets was allowed to include the tolerances observed during manufacturing.

The last step in Fig. 1(a) is an additional selection of the fiber set to maintain the desired distributions from the original 500 measured fibers. Using the modeling approach described above, we expanded the population from 500 elements experimentally measured to 20233 (16467 OM3 and 3766 OM4).

The EMB distributions computed from these populations at

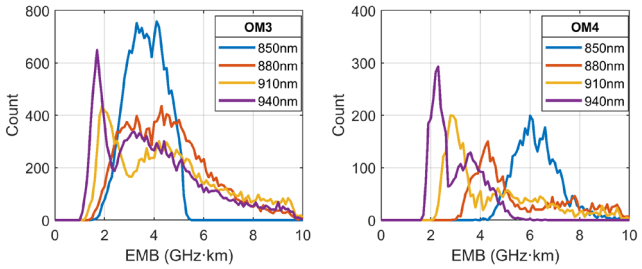

Fig. 2. OM3 and OM4 population EMB distribution at the SWDM wavelengths: 850 nm, 880 nm, 910 nm and 940 nm.

850 nm are shown in Fig. 2 (blue curve). It should be noted that those distributions include some borderline cases slightly below the EMB limits for OM3 and OM4 MMFs (0.66% and 1.38%, respectively) to address observed errors due to DMD measurement tolerances during manufacturing.

The behavior of the EMB for the same fiber population was simulated also at longer wavelengths (880nm, 910 and 940nm) following an approach described in [25], and results are also reported in Fig. 2. Both for OM3 and OM4 we can observe a trend in the reduction of EMB values when increasing the wavelength.

B. VCSEL-MMF coupling and Fiber Transfer Function Model

Once the fibers database was generated, the coupling of the VCSEL to the fiber was modeled using coupling matrices. The coupling matrix (C_{ig}) represents the VCSEL launch condition. Each of the elements of this matrix represents the strength of the coupling between the i_{th} VCSEL mode and the g_{th} fiber mode group. To compute this matrix, the coupling of each VCSEL mode to each guided fiber mode is evaluated using overlap integrals among their field profiles. The coupling strength in each g_{th} fiber mode group is obtained from the quadratic sum of the individual mode's coupling value as described in [2, 26].

The C_{ig} matrix can be used to obtain the spectra of each MMF mode group, PG_g, as follows:

$$PG_g(\lambda) = \sum_{i=1}^{N_{VM}} C_{ig}\, P_i\, \delta(\lambda - \lambda_i) \qquad (4)$$

where P_i is the power in each VCSEL mode. The coefficients C_{ig} can be estimated from spatial-spectral measurements of the light traveling in the core of a MMF. For example, in [26] commercially available VCSELs were coupled to one side of a MMF. From the other side a SMF probe was used to scan the light from MMF at different radial offsets.

In the following we used experimental measurements coming from eight commercial VCSELs mounted on a high-speed test board (4 VCSELs emitting at 850 nm and four VCSELs emitting at 910 nm). The spatially resolved spectrum of the light of four of them is shown in Fig. 3 at different positions inside the core. In these figures, the color represents the central wavelength of the spectrum at each radial position. For each of the spatial positions on the core surface (562 points) we measured the full VCSEL spectrum. These data were used to obtained average spectral distribution at different offset positions, as presented in [26].

The final goal was to merge the MMF characterization (modal delay) and the VCSEL-MMF coupling characterization (PG_g matrixes) to statistically estimate the resulting overall fiber transfer function, using the approach shown in [27]:

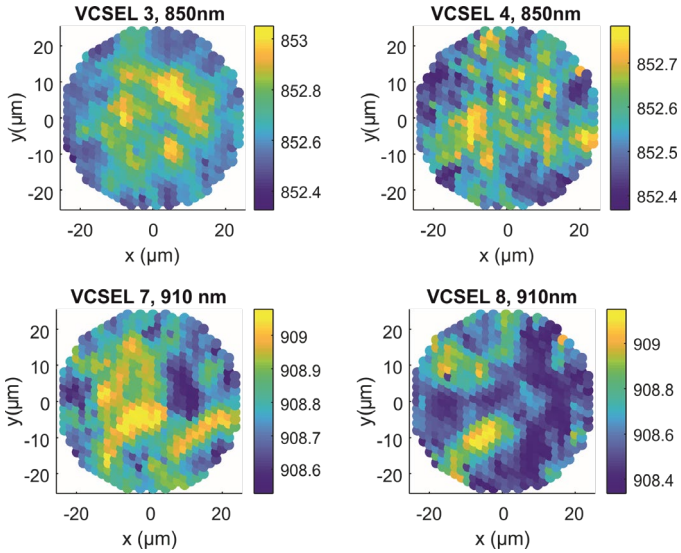

Fig. 3. Spatially resolved spectrum of two 850 nm VCSELs (top) and two 910 nm VCSELs (bottom) at different positions inside the core (the color stands for the central wavelength of the spectrum at each radial position).

$$H_{MMF}(f) = \sum_{g=1}^{N_g} e^{-\alpha_g L} \int_{-\infty}^{\infty} PG_g(\lambda - \overline{\lambda_g}) e^{-i2\pi f \tau_g(\lambda) L} d\lambda \qquad (5)$$

where α_g represents the fiber attenuation of each mode group, τ_g is the group delay described by Eq. (4) and L is the length of the link.

C. VCSEL-MMF Transfer Function Statistics

Based on the model described in previous sub-sections II.A and II.B, we used the previously described database including 8 VCSELs and 20233 MMFs to evaluate the frequency response of all of the possible combinations, obtaining 161864 cases per wavelength and per fiber length.

As we target the analysis of a full SWDM system based on four wavelengths and having a limited set of VCSELs fully characterized in our laboratory (4 working at 850 nm and 4 at 910 nm), we applied an artificial spectral shift to them. Each measured VCSEL, besides being considered at its actual nominal wavelength, it has also been re-used at all other three SWDM wavelengths. This approach allows to have 8 VCSELs sources at all four wavelengths, guaranteeing the same number of analyzed cases. We then assume each VCSEL to have the same spectral properties at all wavelengths.

Moreover, we studied the full system at different fiber lengths within the set [30, 50, 70, 100, 150, 200, 250, 300, 350 and 400] meters. As a result, we simulated a total of 8 (VCSELs) x 4 (wavelengths) x 10 (lengths) x 20233 (fibers) = 6474560 different cases, for each of the two bit-rates analyzed.

Fig. 4 shows an example of the statistical output of our analysis for one laser characterized at 850 nm combined with all the fibers at the four wavelengths, and for a single 100 m fiber length. We plot in Fig. 4(a) the inverse cumulative distribution (i-CDF) of the resulting overall -3 dBo bandwidth. From this i-CDF we can determine the percentage of MMFs that, coupled to a specific VCSEL, have a certain $B\text{-}_{3dB}$. For instance, in the analyzed case, for i-CDF percentages above

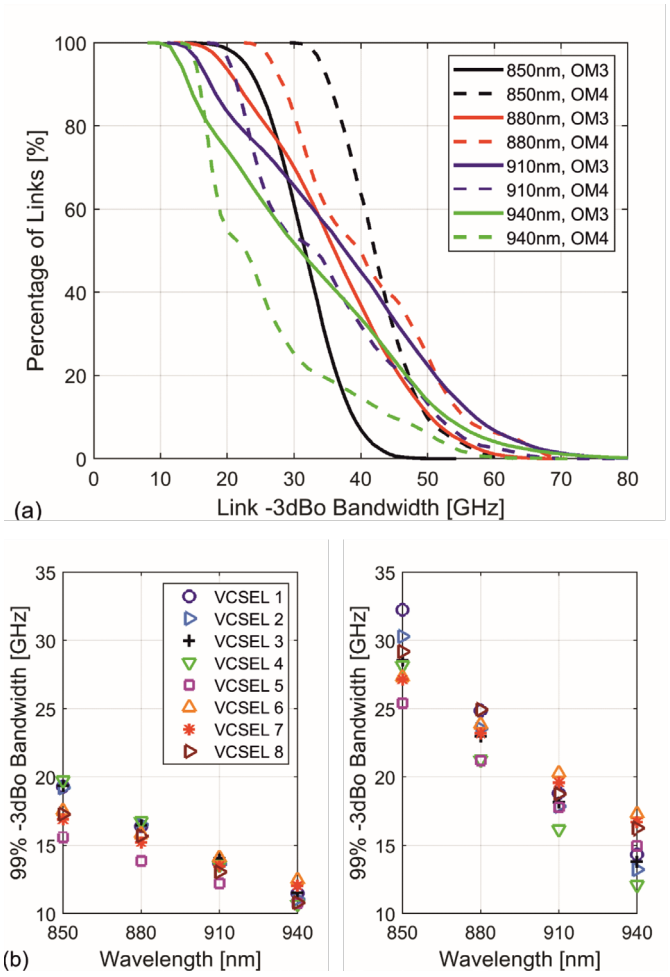

Fig. 4. a) i-CDF of the -3 dBo bandwidth for VCSEL 1 coupled with 100 m OM3 (solid) and OM4 (dashed) fibers at SWDM wavelengths. b) Lower limit of the -3 dBo bandwidth for 99% of the 100m OM3 (left) and 100 m OM4 (right) fibers for all the eight lasers and 4 SWDM wavelengths.

99%, the OM4 fibers (dashed curves) always have a broader $B\text{-}_{3dB}$ than OM3 fibers (solid curves) at the same wavelength. However, the OM4 curves drop quite sharply for increasing $B\text{-}_{3dB}$ showing, for longer wavelengths, a higher percentage of OM4 fibers with narrower bandwidth than OM3 fibers. This can be attributed primarily to the mode group delay distribution of the population, which has a much stronger right tilt for OM4 fibers at long wavelengths as shown in [2].

Since in the following Section we will study statistical system level availability, we show in Fig. 4(b) the $B\text{-}_{3dB}$ lower limit for 99% of the fibers and the eight lasers associated with OM3 and OM4 fiber set at the SWDM wavelengths. It is clear that OM3 fibers provide a lower minimum $B\text{-}_{3dB}$, regardless of the considered transmitting laser. For instance, at 850 nm, 99% of the OM3 fibers have at least 15 GHz $B\text{-}_{3dB}$, whereas OM4 fibers have at least 25 GHz bandwidth when laser number 5 is used (pink squares) and at least 32 GHz $B\text{-}_{3dB}$ when laser 1 is used (blue circles). Moreover, the trends highlight a decreasing $B\text{-}_{3dB}$ at longer wavelengths for both MMF populations, again due to the right tilt effect of the MMFs [2], which increases with the wavelength and prevents chromatic dispersion from counteracting the effect of modal dispersion. This effect, stronger on the OM4 fiber set, almost completely nullifies the advantage of OM4 fibers at 940 nm, where the minimum $B\text{-}_{3dB}$ can be as low as 12 GHz (for laser 4), a level comparable to that obtained for OM3 fibers. We remind here that OM4 have been optimized (to be better than OM3) only at 850 nm, while for having optimized performances on all SWDM wavelengths the newer OM5 MMF fiber class was recently introduced. In our paper, we decide anyway do focus only on OM3 and OM4 because they are by far the most commonly used MMF in datacenter today.

Before proceeding to the performance simulation campaign, as a final check on the extended dataset, we verified that i-CDF distributions of the resulting overall $B\text{-}_{3dB}$ bandwidth have a good match with those obtained considering only the 500 original fibers. This is a good sign that the extension of the fiber population has been done maintaining statistical properties.

III. System Simulation Model

A. Simulation setup

In this sub-section, we describe the system-level numerical simulator used to obtain the core results of this contribution presented in next Section IV. The simulation setup, composed by five main blocks, namely digital transmitter (TX), VCSEL, MMF, optical receiver (PIN+TIA) and digital receiver (RX), is shown in Fig. 5(a). Digital-to-analog (DAC) and analog-to-digital (ADC) converters are added as interfaces between the electro-optical channel blocks and the digital TX and RX, respectively. A variable optical attenuator (VOA) is placed just before the optical RX to set the average received optical power (*ROP*), and thus the receiver optical modulation amplitude (OMA_{RX}).

The digital TX generates a gray-coded PAM-4 signal, with rectangular pulse-shape smoothed by a Gaussian filter with -3 dB frequency equal to 0.75 times the baud rate. The PAM-4 data pattern is generated using random symbols, which change for every simulation run. A FEC overhead is added to the TX sequence. We consider two FEC options: KP4-FEC with 6.25% overhead and $BER_T = 2 \cdot 10^{-4}$, and E-FEC with 10.35% overhead and $BER_T = 4 \cdot 10^{-3}$. Then the raw bit rate is 106.25 Gbps and 110.35 Gb/s when using KP4-FEC and E-FEC, respectively, to have a net post-FEC bit rate of 100 Gbps (50 GBaud).

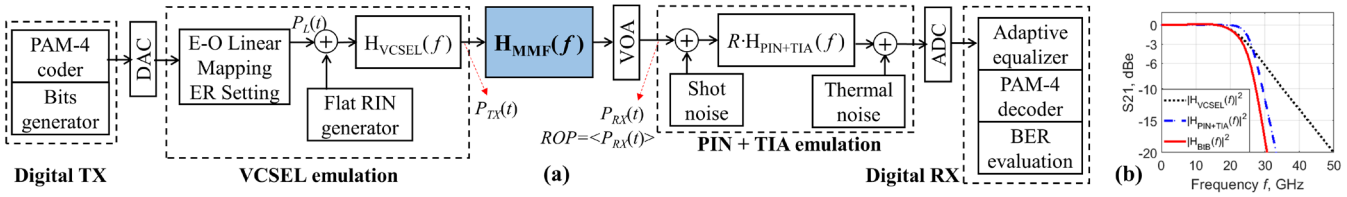

Fig. 5. a) Simulation block diagram (E-O: Electrical to Optical, <·>: mean value operator); b) Electrical frequency response of the VCSEL and PIN+TIA, the back-to-back (BtB) frequency response (in solid red) is the cascade of them.

The PAM-4 DAC output signal drives the VCSEL, which is modeled as a linear device including fixed bandwidth limitations and relative intensity noise addition (RIN). The VCSEL has been assumed as linear because of a twofold reason. First, because good VCSEL sources must be able to work in a bias condition where non-linearity is not relevant. Second, because we are forced to use a simplified model with low complexity running in few seconds per case in order to be able to consider a very large set of conditions for the statistical study (~6.5 million cases). Under these conditions, a linear mapping between the PAM-4 signal and the laser instantaneous power $P_L(t)$ is performed to set the desired average laser output power $\langle P_{TX}(t) \rangle$ and the target extinction ratio (ER) of the optical modulated signal. The RIN is generated as a white Gaussian noise random process with variance $\sigma_{RIN}^2 = (P_L(t))^2 \cdot \Gamma_{RIN} \cdot B_S$, where Γ_{RIN} is the RIN coefficient in 1/Hz (referred to the carrier) and B_S is the one-sided simulation bandwidth in Hz (twice the baud rate). The RIN is added to $P_L(t)$ and the resulting noisy signal is filtered by the VCSEL frequency response $H_{VCSEL}(f)$. The signal that outputs the $H_{VCSEL}(f)$ block is the instantaneous transmitted power $P_{TX}(t)$.

Two system configurations can be set: back-to-back (BtB) and MMF propagation. In the BtB one, the $P_{TX}(t)$ signal inputs directly the VOA. In the MMF propagation case, an $H_{MMF}(f)$ filter is applied to the instantaneous power signal $P_{TX}(t)$. The MMF block generates the transfer function $H_{MMF}(f)$ that models the VCSEL-MMF coupling and the signal propagation through the MMF as described in detail in previous Section II [2]. A chromatic-dispersion coefficient D = -103, -91, -79 and -69 ps/nm·km is set for λ = 850, 880, 910 and 940 nm, respectively, as given in ITU-T G.651 standard.

At the receiver side, after setting the proper ROP (see Table I), the signal is detected by the PIN+TIA optical receiver. In the PIN+TIA model employed here, shot noise is added to the instantaneous PIN input optical power $P_{RX}(t)$, the resulting signal is multiplied by the responsivity factor R and then filtered by the PIN+TIA frequency response $H_{PIN+TIA}(f)$. Finally, thermal noise (accounting for the TIA noise, which usually ends up being the most relevant noise source for these systems) is added to the filtered signal. The shot and thermal noise sources are modeled as additive white Gaussian noise random processes, with variance evaluated as follows: $\sigma_{sh}^2 = 2qB_sP_{RX}(t)$ and $\sigma_{th}^2 = B_s \cdot (IRND)^2$ respectively. $IRND$ is the intensity relative noise density and q is the electron charge. The electrical signal at the output of the optical receiver is down-sampled to 2 samples per symbol (SpS), emulating the analog-to-digital conversion at the receiver. As it is know from the literature on equalizers (see for instance [28] Chapter 10), a 2 SpS equalizer without optimization of the sampling instant (as assumed here) has basically the same performance of a 1 SpS equalizer with optimal sampling clock recovery (which is the solution of choice used in high-speed equalizers today for MMF systems).

Finally, the digital received signal is DSP processed using one of the following three schemes: *i*) a Feed Forward Equalizer (FFE), *ii*) a combination of FFE followed by a Distributed Feedback Equalizer (DFE) (approach termed just as "DFE" in the following for simplicity), and *iii*) a Maximum- Likelihood Sequence Estimation (MLSE)-based equalizer preceded by a proper channel shortening filter. FFE and DFE work at 2 SpS (i.e. T/2-Spaced) and 1 SpS (T-Spaced), with 20 and 5 taps, respectively. Both FFE and DFE are first trained with 10^4 symbols using the Least-Mean-Square (LMS) algorithm, and then their operation is switched to the tracking (i.e. decision-directed) mode. Fixed adaptation coefficients $\mu_1 = 10^{-3}$ and $\mu_2 = \mu_1/2$ are used in the training and tracking modes, respectively (the signal is normalized to unity power at the input of the equalizers). Regarding MLSE-based equalization, the following algorithms are serially applied [29]: *i*) channel estimation, working at 2 SpS with 50 taps using the adaptive LMS algorithm, trained with 10^4 symbols, *ii*) channel shortening, working at 2 SpS with 50 taps for Time Domain Equalization (TDE), and 4 taps for the Target Impulse Response (TIR), and *iii*) an MLSE Viterbi algorithm, using 2^4 states, working at 2 SpS with fixed adaptation coefficient $\mu = 10^{-4}$ and trained with $2 \cdot 10^4$ symbols. After equalization, PAM-4 decision and decoding follows. Finally, the bit error rate (BER) is evaluated through direct error counting over ~10^5 bits, not including in the BER computation the bits used for equalizer training.

The magnitude of the VCSEL and PIN+TIA frequency responses set in the SWDM simulator, $H_{VCSEL}(f)$ and $H_{PIN+TIA}(f)$, respectively, are plotted in Fig. 5(b). They were directly extrapolated (after a frequency domain smoothing) from standard 25G-class devices. The cascade of these two transfer functions is also shown as the red curve of Fig. 5(b), termed as the back-to-back (BtB) transfer function $H_{BtB}(f)$. A -3 dB full-system electrical bandwidth of 23 GHz is measured in BtB conditions.

B. Back-to-back simulation performance

An evaluation of the system under analysis is first performed in BtB, varying the raw transmitted bit rate around the values analyzed in this work (i.e. 106.25 and 110.35 Gbps), using the TX and RX parameters shown in Table I.

In Fig. 6, BER as a function of raw bit rate is reported for all three equalizers. In dashed lines we indicate the two BER_T values. Using FFE, 116 Gbps and 124 Gbps transmission can be achieved in BtB using KP4-FEC and E-FEC, respectively. Both DFE and MLSE provide a performance gain with respect to FFE for the bit rates under analysis (MLSE outperforming DFE). For bit rates equal or lower than 105 Gbps, the 3 equalizers offer very similar performance. At 106.25 Gbps (110.35 Gbps), a BtB BER of {$3 \cdot 10^{-6}$, $3 \cdot 10^{-6}$ and $4 \cdot 10^{-6}$} ({$5 \cdot 10^{-6}$, $7 \cdot 10^{-6}$ and $12 \cdot 10^{-6}$}) is obtained for {FFE, DFE and MSLE}, showing in both cases a BER margin to include fiber propagation up to a given distance to be statistically analyzed.

IV. Statistical Analysis of SWDM systems

In this Section, we present the extensive statistical analysis that is the core of our paper. In particular, we focus on the maximum reach of a 100 Gbps PAM-4 DCI transmission system, over the

TABLE I. SIMULATION PARAMETERS USED FOR STATISTICAL ANALYSIS OF SWDM SYSTEMS

Parameter	Value	Units
ER	3.0	dB
RIN coefficient, Γ_{RIN}	-141.0	dBc/Hz
Received OMA, OMA_{RX}	-3.5	dBm
Received Optical Power, ROP	-1.75	dBm
$IRND$	20.0	pA/sqrt(Hz)
R	0.5	A/W

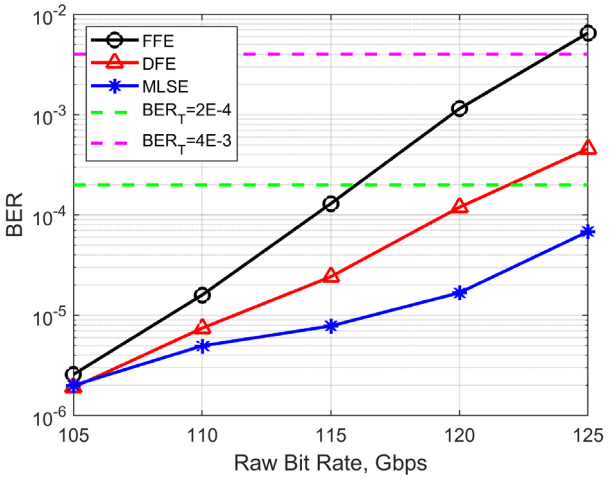

Fig. 6 PAM-4 BtB BER as a function of raw bit rate, for different equalizers, using the system parameters shown in Table I.

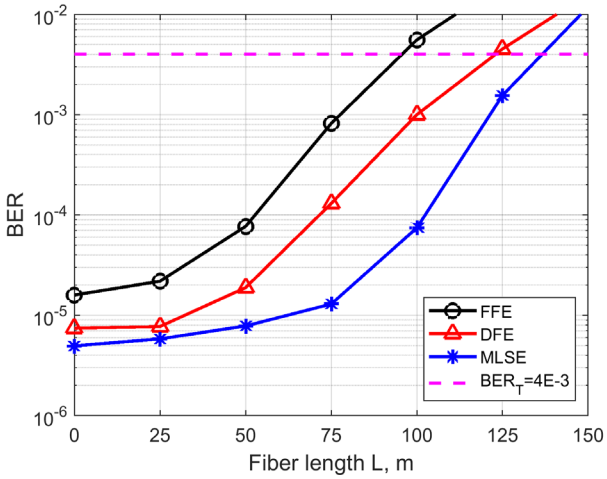

Fig. 7 PAM-4 110.35 Gbps BER as a function of fiber length, for different equalizers, using the system parameters shown in Table I. The analyzed fiber was selected from the OM3 data set in combination with VCSEL 1.

large VCSEL-MMF dataset introduced in Section II. Using the simulation tool presented in Section III (schematically depicted in Fig. 5) and setting the parameters shown in Table I, we compute the maximum reach (L_{max}) of each of the 647456 available cases (8 VCSELs x 20233 MMFs x 4 λs) per bit rate.

A. Analysis of a sample VCSEL-MMF of the dataset

In this sub-section, we introduce the methodology of the analysis. Our goal is to evaluate for each single case (VCSEL, MMF and wavelength), the L_{max} metric. As an example, in Fig. 7, we report results for one OM3 sample coupled with VCSEL #1. The case under analysis has a fiber EMB = 1.968 GHz-km, and a VCSEL-MMF $B\text{-}_{3dB}$ = 19.5 GHz (for a length of 100 m). The bit rate selected for this analysis is 110.35 Gbps.

Following the model presented in Section II, we compute the transfer function of the VCSEL-MMF sample for a set of discrete fiber lengths, and evaluate the corresponding BER performance. In Fig. 7, BER versus fiber length curves are shown for different equalizers. The E-FEC BER_T is shown in dashed line. The maximum reach (L_{max}) at the BER_T is obtained by linear interpolation. In this sample case, L_{max} = {95 m, 124 m, 137 m} for {FFE, DFE, MLSE}.

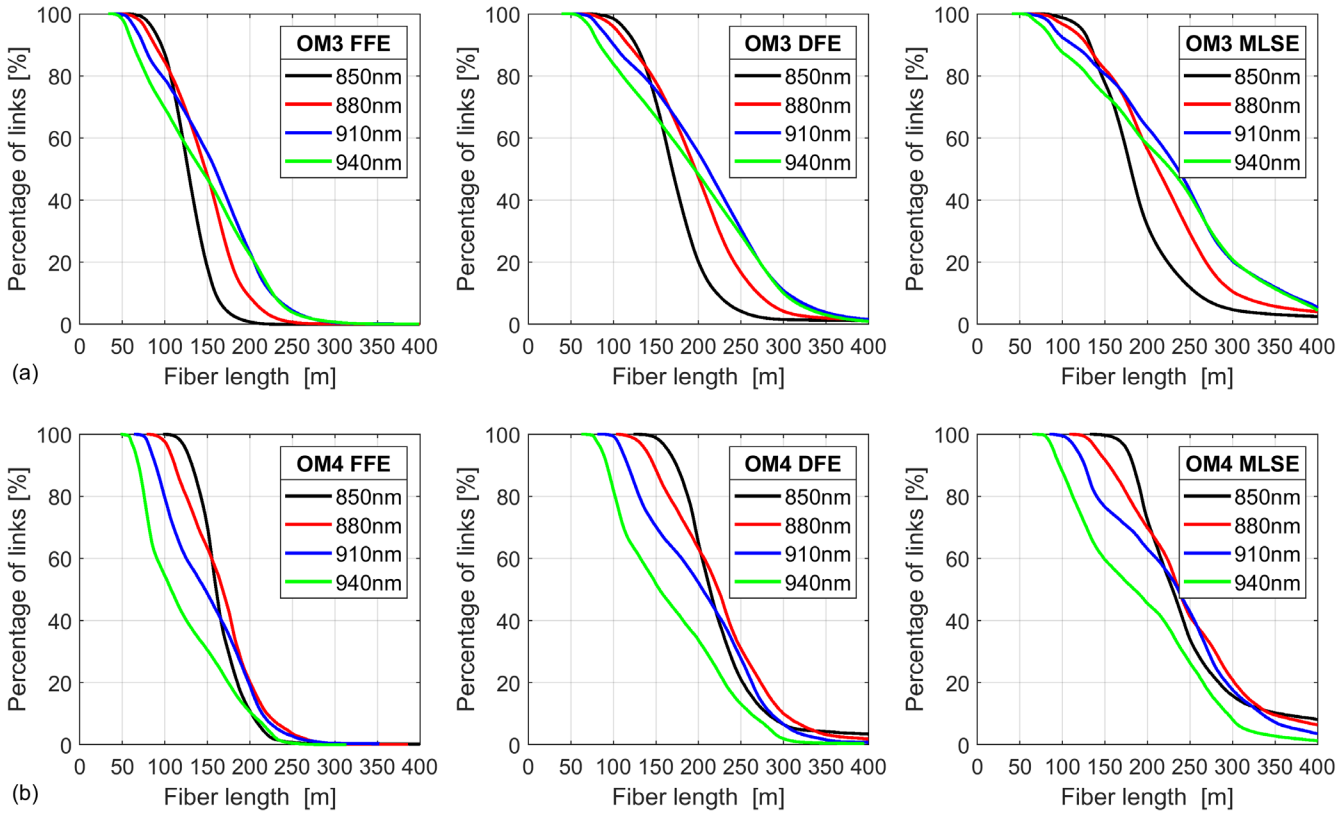

Fig. 8. Inverse CDF (in percentage) of 110.35 Gbps links working at or below the E-FEC threshold as a function of the MMF length for the three equalizers at SWDM wavelengths 850 nm (black), 880 nm (red), 910 nm (blue) and 940 nm (green) for a) OM3 and b) OM4 fibers.

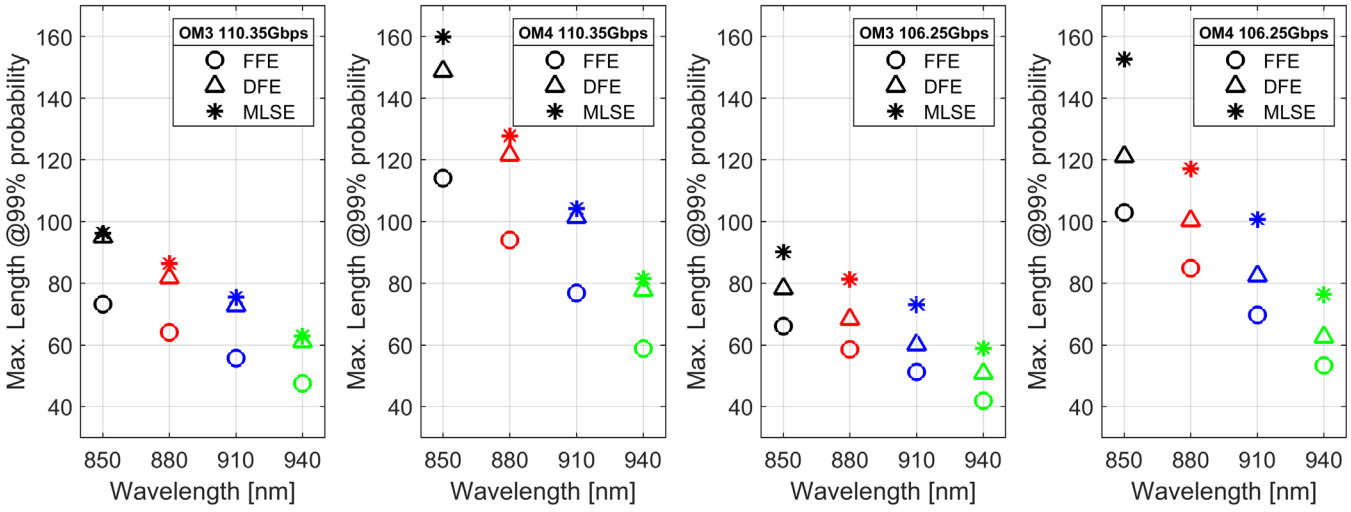

Fig. 9 Achievable reach for 99% of the 100G links at the 4 SWDM wavelengths 850 nm (black), 880 nm (red), 910 nm (blue) and 940 nm (green) for KP4-FEC (left) and E- FEC (right) thresholds, and for the 3 equalizers for both OM3 and OM4 fiber sets.

B. Statistical analysis of the whole VCSEL-MMF dataset

By repeating the procedure indicated in the previous sub-section, for all the available VCSEL-MMF cases, we evaluated the maximum reachable distance L_{max} for each combination of fiber, distance, wavelength, FEC and equalizer. Fig. 8 shows the resulting inverse cumulative distribution functions (i-CDF) of L_{max} on the links working below the E-FEC threshold (thus allowing to use a raw data rate of 110.35 Gbps) as a function of the MMF length, for the four SWDM wavelengths (in different color) and for the three equalizers (in different graphs). The three graphs at the top (bottom) are for OM3 (OM4) fiber subsets.

From Fig. 8, we can observe the following trends. There is a performance worsening when increasing λ, which is quite striking, especially for the OM4 fibers subset (and for OM3 considering link feasibility above 50% of the whole set). This result is aligned with the i-CDF of the $B\text{-}_{3dB}$ shown in Fig. 4. For all wavelengths and type of fibers, there is a clear performance ranking among the equalizers: MLSE > DFE > FFE, as expected. It is interesting to note that the i-CDFs for different wavelengths cross as increasing the fiber length (for same equalizer and same type of MMF), which is due to a tradeoff between fiber bandwidth and chromatic dispersion: in general, the shorter the wavelength the larger the EMB (as shown in Fig. 2). Conversely, the absolute value of the dispersion coefficient decreases with wavelength.

When comparing the OM3 and OM4 i-CDF curves (irrespective of the equalizer), we can observe that OM4 one outperform OM3 irrespective of the distance operating at 850 nm. Conversely, OM3 shows better performance than OM4 operating at 940 nm. This can be anticipated by looking at the EMB distributions of Fig. 2. While most of the OM4 fibers have higher EMB than OM3 ones at 850 nm, the opposite trend is observed at 940 nm. The intermediate wavelengths exhibits a behavior in between. We remind here that OM3 and OM4 are not optimized for SWDM but they were originally developed for use at 850 nm, whereas newer OM5 MMF have specifically been designed for SWDM.

From the i-CDF graphs shown in Fig. 8, the reach L_{max} that a given percentage of the 100G links can achieve is evaluated. Fig. 9 shows, for the two bit rates and all λs and equalizers, the maximum reach that can be achieved by 99% of the links. The decreasing trend with λ shown in Fig. 4 for the $B\text{-}_{3dB}$ is observable also on L_{max}, with the 940 nm case limiting the overall 100G SWDM system to ~60 m for OM3 fibers with E-FEC+MLSE or KP4-FEC+MLSE and ~80 m for OM4 fibers with E-FEC+MLSE and KP4-FEC+MLSE. However, transmission at 850 nm can be successfully provided by 99% of the fibers in our dataset with a reach limit of around 70 m for OM3 fibers and 110 m for OM4 fibers using E-FEC+FFE. At 850 nm, a simpler KP4-FEC+FFE provides a reach ~100 m using OM4. These reaches meet the requirements targeted by the new standards.

As a final comparison, Fig. 10 summarizes in a single graph the most relevant results of our paper, showing the achievable reach L_{max} for 99% of the 100G links at the 4 SWDM

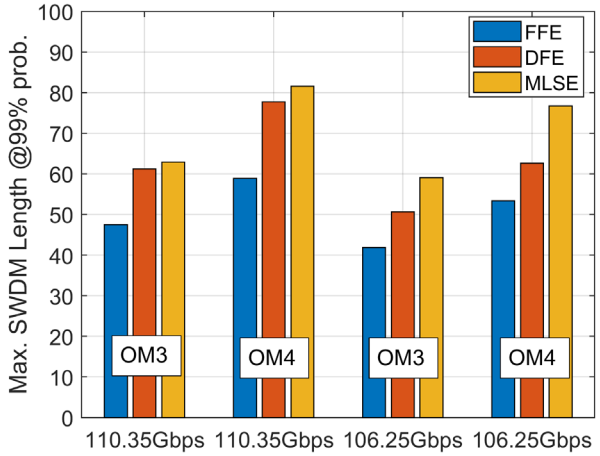

Fig. 10. Comparison of the achievable SWDM reach for 99% of the 100G links for E-FEC and KP4-FEC thresholds, and for the three equalizers.

wavelengths for both considered FEC thresholds. Mostly limited by the 940 nm case, the SWDM maximum reach is 80 m using OM4 fibers, MLSE and E-FEC. Regarding OM3, at least 50 m can be achieved with both FECs and using DFE or MLSE. Overall, the 110.35 Gbps E-FEC approach outperforms the KP4-FEC one for both OM3 and OM4 fibers, irrespective of the equalization scheme.

V. Conclusions

Based on a large dataset of MMF fibers and VCSEL sources, we have statistically evaluated the performance of VCSEL-MMF systems at 100 Gbps/λ in a SWDM scenario. Our results indicate that future 100G Ethernet data rates per wavelength are feasible for up to 120 m of OM4 at 850 nm using DFE. Aggregated data rates of 400 Gbps per fiber using SWDM grid are achievable but for shorter reaches (~80 m OM4 + MLSE). However, there is no need to use the full grid to expand significantly the data rates. For example, using only two λs: 850 nm and 910 nm, in a bidirectional approach similar to the one adopted in 400GBASE.SR4.2, 200 Gbps for up to ~80 m can be enabled using FFE. A more complex receiver, a stronger FEC and pre-distortion (not shown in this paper) could further increase the reaches.

Acknowledgment

The authors acknowledge HPC @ POLITO (http://www.hpc.polito.it/) for providing the high-performance computational resources used in this work.

References

[1] D. M. Kuchta, "High Capacity VCSEL-based links," Optical Fiber Communication Conference, OSA Technical Digest (online) (Optical Society of America, 2017), paper Tu3C.4.

[2] J. M. Castro, R. Pimpinella, B. Kose and B. Lane, "Investigation of the Interaction of Modal and Chromatic Dispersion in VCSEL–MMF Channels," Journal of Lightwave Technology, vol. 30, no. 15, pp. 2532-2541, 2012.

[3] J. M. Castro, R. Pimpinella, B. Kose, P. Huang, A. Novick and B. Lane, "Modal-Chromatic Dispersion Interaction Effects for 850 nm VCSEL Channels at 100 Gb/s per Wavelength," Journal of Lightwave Technology, vol. 39, no. 7, pp. 2067-2076, 2021.

[4] R. Murty, "Summary of Technical Feasibility Demonstrated for 100 m OM4 MMF Links," IEEE P802.3db 100 Gb/s, 200 Gb/s, and 400 Gb/s Short Reach Fiber Task Force Ad Hoc Teleconference, November 10, 2020. [Online] Available: https://www.ieee802.org/3/db/public/November20/murty_3db_01a_1120.pdf

[5] J. M. Castro, *et al*, "Initial considerations for 100G VCSEL MMF reaches", 100 Gb/s Wavelength Short Reach PHYs Study Group Geneva, Switzerland Jan 2020. [Online] Available: https://www.ieee802.org/3/100GSR/public/Jan20/castro_100GSR_01a_120.pdf

[6] S. E. Ralph and J. Lavrencik, "High Capacity VCSEL Links," Optical Fiber Conference (OFC), 2019, pp. 1-3.

[7] IEEE 802.3cm, 400 Gb/s over Multimode Fiber Task Force Public Area, http://www.ieee802.org/3/cm/public/index.html

[8] J. A. Tatum et al., "VCSEL-Based Interconnects for Current and Future Data Centers," in Journal of Lightwave Technology, vol. 33, no. 4, pp. 727-732, 2015.

[9] "100G-SWDM4 MSA Technical Specifications" http://www.swdm.org/wp-content/uploads/2017/11/100G-SWDM4-MSA-Technical-Spec-1-0-1.pdf

[10] E. Parsons, M. Lanier, R. Patterson and G. Irwin, "100G SWDM Transmission over 250m OM5 and OM4+ Multimode Fibers," 2018 Optical Fiber Communications Conference and Exposition (OFC), San Diego, CA, 2018, pp. 1-3.

[11] I. Lyubomirsky *et al*., "100G SWDM4 transmission over 300m wideband MMF," 2015 European Conference on Optical Communication (ECOC), Valencia, 2015, pp. 1-3.

[12] C. Kocot et al., "SWDM strategies to extend performance of VCSELs over MMF," 2016 Optical Fiber Communications Conference and Exhibition (OFC), Anaheim, CA, 2016, pp. 1-3.

[13] Y. Sun et al., "SWDM PAM4 Transmission Over Next Generation Wide-Band Multimode Optical Fiber," in Journal of Lightwave Technology, vol. 35, no. 4, pp. 690-697, 15 Feb.15, 2017.

[14] L. Chorchos et al., "Energy Efficient 850 nm VCSEL Based Optical Transmitter and Receiver Link Capable of 80 Gbit/s NRZ Multi-Mode Fiber Data Transmission," in Journal of Lightwave Technology, vol. 38, no. 7, pp. 1747-1752, 1 April1, 2020.

[15] F. Karinou, N. Stojanovic, C. Prodaniuc, Z. Qiang and T. Dippon, "112 Gb/s PAM-4 Optical Signal Transmission over 100-m OM4 Multimode Fiber for High-Capacity Data-Center Interconnects," ECOC 2016; 42nd European Conference on Optical Communication, Dusseldorf, Germany, 2016, pp. 1-3.

[16] T. Zuo, L. Zhang, E. Zhou, G. N. Liu and X. Xu, "112-Gb/s duobinary 4-PAM transmission over 200-m multi-mode fibre," 2015 European Conference on Optical Communication (ECOC), Valencia, Spain, 2015, pp. 1-3

[17] C. Kottke, C. Caspar, V. Jungnickel, R. Freund, M. Agustin, and N. N. Ledentsov, "High Speed 160 Gb/s DMT VCSEL Transmission Using Pre-equalization," in Optical Fiber Communication Conference, OSA Technical Digest (online) (Optical Society of America, 2017), paper W4I.7.

[18] R. Puerta et al., "Effective 100 Gb/s IM/DD 850-nm Multi- and Single-Mode VCSEL Transmission Through OM4 MMF," in Journal of Lightwave Technology, vol. 35, no. 3, pp. 423-429, 1 Feb.1, 2017.

[19] Xiaohe Dong, Nikos Bamiedakis, David George Cunningha m, Richard Vincent Penty, and Ian Hugh White, "A Novel Equalizer for 112 Gb/s CAP-Based Data Transmission Over 150 m MMF Links," J. Lightwave Technol. 37, 5937-5944 (2019).

[20] IEEE P802.3db 100 Gb/s, 200 Gb/s, 400 Gb/s Short Reach Fiber Task Force Public Area, https://www.ieee802.org/3/db/index.html

[21] J. Lavrencik et al., "4λ × 100Gbps VCSEL PAM-4 transmission over 105m of wide band multimode fiber," 2017 Optical Fiber Communications Conference and Exhibition (OFC), Los Angeles, CA, 2017, pp. 1-3.

[22] TIA-455-220-A, Differential Mode Delay Measurement of Multimode Fiber in the Time Domain, Telecommunication Industry Association, 2003.

[23] D. Schicketanz, "Fitting of a Weighted Gaussian Lowpass Filter to the Transfer Function of Graded-Index Fibres to Reduce Bandwidth Ambiguities", Elec. Lett. 19 (17), pp. 651-652, 1983.

[24] TIA contribution TR42.12-2018-06-008, presented to TIA TR42.12 subcommittee, June 2018 meeting, Pittsburg, PA, 2018.

[25] J. M. Castro, et al., "Spectral Dependence of Multimode Fiber M odal Bandwidth," Eur. Conf. Opt. Comm. (ECOC), 2018, pp. 1-3

[26] J. M. Castro, R. Pimpinella, B. Kose, P. Huang, A. Novick and B. Lane, "Modal-Chromatic Dispersion Interaction Effects for 850 nm VCSEL Channels at 100 Gb/s per Wavelength," in Journal of Lightwave Technology, vol. 39, no. 7, pp. 2067-2076, 1 April1, 2021, doi: 10.1109/JLT.2020.3046741.

[27] G. Yabre, "Comprehensive Theory of Dispersion in Graded-Index Optical Fibers," IEEE-OSA JLT.18, 166-177, Feb. 2000.

[28] J. Proakis, M. Salehi, Digital Communications, 5th edition, Mc-Graw Hill, ISBN 978–0–07–295716–7

[29] N. Al-Dhahir, J. M. Cioffi, " Efficiently computed reduced-parameter input-aided MMSE equalizers for ML detection: a unified approach IEEE Transac. Info. Theory, 42 (3), pp. 903-915, 1996.